# Energy Delay Tradeoff in Multichannel Full-Duplex Wireless LANs

Zhefeng Jiang, *Student Member, IEEE*, and Shiwen Mao, *Senior Member, IEEE*

***Abstract*—Although full-duplex transmission can be helpful for enhancing wireless link capacity, it may require extra energy to overcome the residual self-interference. In this paper, we investigate the tradeoff between energy consumption and delay in a multichannel full-duplex wireless LAN. The goal is to minimize the energy consumption while keeping the traffic queues stable. With Lyapunov optimization, we develop a throughput optimal online scheme to achieve the goals with optimized channel assignment, transmission scheduling, and transmission mode selection. We study the influence of full-duplex transmissions on the network capacity region, prove the optimality of the proposed algorithm, and derive upper bounds for the average queue length and energy consumption, which demonstrate the energy-delay tradeoff in such systems. The proposed algorithm and the capacity region analysis are validated with simulations.**

***Index Terms*—Capacity region, energy efficiency, full-duplex, Lyapunov optimization, wireless LAN (WLAN).**

## I. Introduction

DUE TO the dramatic increase of wireless data demand, as driven by the wide use of smartphones, tablets and other smart devices, there is an urgent need to improve the spectrum efficiency of existing wireless networks. Through effective self-interference cancellation, full-duplex transmission, i.e., transmitting and receiving simultaneously in the same band, has been successfully demonstrated [1], [2]. With various self-interference cancellation techniques, full-duplex transmission has the potential to increase and even double the wireless link capacity [3].

Combined with RF interference cancellation and digital baseband interference cancellation, antenna cancellation can effectively suppress the self-interference for full-duplex transmission. In [3]–[5], analog and digital cancellation techniques were investigated. With full-duplex transmissions, various full-duplex links can be formed. For example, in the three-node full-duplex link scenario, one node (e.g., a base station) executes self-interference cancellation to transmit to and receive from two different half-duplex nodes simultaneously [6], [7]. In the two-node link scenario, both nodes are capable of self-interference cancellation and can transmit to and receive from each other simultaneously [8]–[11].

Due to imperfect self-interference cancellation, the residual self-interference may still lead to a lower signal-to-interference-plus-noise ratio (SINR) and deteriorate the performance of a full-duplex link [12]. Additional power is thus needed to combat the residual self-interference to achieve a suitable SINR. As a result, full-duplex transmission may not always be helpful, and there is a tradeoff between the energy cost and delay in the design of full-duplex wireless networks [13]. In [12] and [13], the extra energy consumption and the limits of full-duplex transmission were investigated. Joint resource allocation and scheduling in wireless networks is a challenging problem, for which Lyapunov optimization has been applied and shown effective [14]–[17]. However, these prior works are all focused on half-duplex wireless networks. Many challenging issues that arise in full-duplex wireless networks have not been adequately addressed.

In this paper, we consider a multichannel wireless LAN (WLAN) where both access point (AP) and nodes are capable of full-duplex transmission. Since full-duplex is not always more efficient than half-duplex, we aim to jointly consider the problems of channel assignment, transmission scheduling, and transmission mode selection for the AP and nodes. We develop a problem formulation to capture the tradeoff between energy consumption and queue length (which is indicative of delay) in the multichannel full-duplex WLAN, with the objective to minimize the overall energy consumption of the system and stabilize the packet queues at all the nodes. We provide an analysis of the capacity region of full-duplex systems, which encompasses the capacity region of the corresponding half-duplex system. We then develop an effective solution algorithm based on the Lyapunov optimization framework. With the proposed algorithm, the overall optimization problem over the entire time period is first reduced to the minimization of a *drift-plus-penalty* for each node in each time slot. The reduced problem only depends on the queue lengths, wireless link rates, and energy consumptions in the current time slot. We then transform the reduced problem into a maximum weighted matching problem and solve it with the Hungarian method with a polynomial complexity [18].

The proposed algorithm is an online algorithm since it does not require any past and future information of the

Manuscript received September 24, 2016; revised November 24, 2016; accepted December 6, 2016. Date of publication December 13, 2016; date of current version June 15, 2017. This work was supported by the U.S. National Science Foundation through the Wireless Engineering Research and Education Center, Auburn University under Grant CNS-1247955. This paper was presented in part at the 10th International Conference on Wireless Algorithms, Systems, and Applications, Qufu, China, August 2015.

Z. Jiang was with the Department of Electrical and Computer Engineering, Auburn University, Auburn, AL 36849-5201 USA. He is now with Google Inc., Mountain View, CA 94043 USA (e-mail: zzj0007@tigermail.auburn.edu).

S. Mao is with the Department of Electrical and Computer Engineering, Auburn University, Auburn, AL 36849-5201 USA (e-mail: smao@ieee.org).

Digital Object Identifier 10.1109/JIOT.2016.2638851

WLAN system. We prove that the proposed algorithm minimizes the *drift-plus-penalty* among all possible transmission modes and channel assignment schemes. Furthermore, we derive upper bounds on the average sum queue length and average total energy consumption under the proposed algorithm, which demonstrate the energy-delay tradeoff in the multichannel full-duplex WLAN. The performance of the proposed algorithm is validated with simulations.

This paper is organized as follows. We review related work in Section II. The system model and problem formulation are presented in Section III. The capacity region is studied in Section IV. The proposed algorithm is developed and analyzed in Section V. Our simulation study is presented in Section VI. Section VII concludes this paper.

## II. Related Work

The potential of full-duplex transmissions on a single channel was investigated in [2], [19], and [20]. Combined with RF interference cancellation and digital baseband interference cancellation, antenna cancellation can achieve sufficient self-interference cancellation for full-duplex operation [2]–[5], [21], [22]. In [2], self-interference suppressing with multiantenna is exploited. In [21], ideas of increasing analog/RF isolation were proposed to enhance self-interference cancellation and allow compact radio design. In [3]–[5] and [22] analog and digital cancellation techniques were studied to enhance self-interference cancellation. There are two types of wireless full-duplex transmissions. In the first type of full-duplex transmission, three nodes are involved. In this case, only one node operates interference cancellation which transmit and receive at the same time, while the other two nodes operating on half-duplex mode. In the later type of full-duplex transmission, two nodes are involved and both are transmitting and receiving at the same time [8], [9]. In this paper, the two-node full-duplex transmission scenario is considered.

Full-duplex transmission has been studied in relay networks as a mean of acquiring additional resources [23]–[29]. To fully utilize the potential benefits of full-duplex radios, network-level mechanisms were also studied to apply full-duplex transmissions into different systems. To incorporate full-duplex into WLANs, where MAC protocols were designed for Half-duplex radios, new MAC protocols were designed to allow full-duplex transmissions [12], [30]–[36]. Zhou *et al.* [32] presented a signaling mechanism based on pseudo-random noise sequences to enable multimodal operation of wireless links in a distributed channel access setting. The goal was to identify and support concurrent transmissions in the neighborhood.t adopts the pseudo-random links on-the-fly and explore the chance of exposed transmissions In [12], a hybrid scheduler was presented, which defaulted to half-duplex operation but can assign full-duplex time slots when it was advantageous to do so. Kim *et al.* [34] explored the packet-alignment-based capture effect for concurrent transmission between the AP and two different clients, which can be fitted into scenarios that only the AP is full-duplex enabled. The secrecy performance of full-duplex relay networks was also studied in [35], which showed that secrecy performance in relay networks can be significantly improved with full duplex jamming schemes.

There have been only a few works addressing the scheduling, resource allocation, and capacity region of full-duplex systems in orthogonal frequency division multiple access (OFDMA) multichannel networks. For half-duplex systems, scheduling and resource allocation were studied in many prior works, where the energy-capacity tradeoff was derived [37] and the energy-delay tradeoff was investigated in [38]. Resource allocation and channel assignment in OFDMA has been extensively exploited [14], [15], [39], [40], In [14] and [15], scheduling and resource allocation decisions were addressed by minimizing queue length under an energy consumption constraint based on Lyapunov optimization. In [17], a framework of the Lyapunov optimization was proposed to balance the energy consumption and queue length. In [41], a subcarrier assignment and power allocation scheme was proposed to maximize the sum-rate performance. In addition, Due to imperfect self-interference cancellation, full-duplex is not always better than half-duplex [8], [9], [11]. In [12], [13], and [20], the extra energy consumption and the limits of full-duplex were examined.

However, these works either did not take into account of the arrival of packets at different nodes or only worked for half-duplex systems. Hence, in this paper, we present a study of the full-duplex and half-duplex model selection, and the related scheduling and resource allocation decisions in multichannel, multiuser networks. The impact of full-duplex transmissions on the system capacity region will also be investigated.

## III. System Model and Problem Statement

### A. System Model

The system model is illustrated in Fig. 1. We consider a WLAN with one AP, a set of nodes denoted as $\mathcal{N} = \{1, 2, \ldots, N\}$, and a set of orthogonal channels denoted as $\mathcal{S} = \{1, 2, \ldots, S\}$. The AP determines the channel assignment, transmission schedule, and transmission mode selection for both uplink and downlink transmissions. We assume that data is transmitted via the AP in packets, and there is no direct transmission among the nodes. The packets waiting for transmission are buffered and served in the first in first out manner. We assume a discrete time system. The uplink queue backlogs at the beginning of time slot $t$ are denoted as $\vec{Q}^u(t) = \{Q_1^u(t), Q_2^u(t), \ldots, Q_N^u(t)\}$ and the downlink queue backlogs are denoted as $\vec{Q}^d(t) = \{Q_1^d(t), Q_2^d(t), \ldots, Q_N^d(t)\}$, where $Q_i^u(t)$ is the backlog of the uplink queue maintained at node $i$ and $Q_i^d(t)$ is the backlog of the downlink queue for node $i$ maintained at the AP.

At time slot $t$, the arrivals of packets to the uplink queues are denoted as $\vec{A}^u(t) = \{A_1^u(t), A_2^u(t), \ldots, A_N^u(t)\}$. The arrivals of packets to the downlink queues are denoted as $\vec{A}^d(t) = \{A_1^d(t), A_2^d(t), \ldots, A_N^d(t)\}$. In addition, we assume that the arrivals of packets, either to the uplink or downlink queues, are i.i.d. over time. Note that analysis in this paper is general and does not require an specific arrival processes.

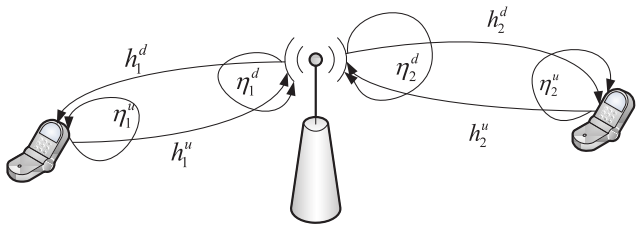


Fig. 1. Illustration of the multichannel full-duplex WLAN with two mobile devices and two channels.

The expectations, i.e., the average arrival rates, are

$$\vec{\lambda}^u \triangleq \mathbb{E}\left\{\vec{\mathcal{A}}^u(t)\right\} = \left\{\lambda_1^u, \lambda_2^u, \ldots, \lambda_N^u\right\} \tag{1}$$

$$\vec{\lambda}^d \triangleq \mathbb{E}\left\{\vec{\mathcal{A}}^d(t)\right\} = \left\{\lambda_1^d, \lambda_2^d, \ldots, \lambda_N^d\right\}. \tag{2}$$

Recall that there are $\mathcal{S} = \{1, 2, \ldots, S\}$ orthogonal channels. During each time slot $t$, a node can transmit and/or receive on one of the channels in $\mathcal{S}$. The channel assignment decision for each node $i$ is denoted as $\alpha_i(t)$, where $i \in \mathcal{N}$ and $\alpha_i(t) \in \{\mathcal{S} \cup \{0\}\}$ is the channel node $i$ uses at time slot $t$. Note that $\alpha_i(t) = 0$ indicates that no channel is assigned to node $i$. In addition, each node can choose from three transmission modes: *uplink*, *downlink*, or *full-duplex*. The transmission mode selection is denoted as $\beta_i(t) \in \{U, D, F\}$, where $\beta_i(t) = U$, $\beta_i(t) = D$, and $\beta_i(t) = F$ indicate that at time slot $t$, node $i$ selects half-duplex uplink, half-duplex downlink, and full-duplex transmission, respectively.

For the full-duplex mode, the residual self-interference is treated as interference. Let $C_i^u(t)|_{\alpha_i(t)=s,\beta_i(t)=F}$ and $C_i^d(t)|_{\alpha_i(t)=s,\beta_i(t)=F}$ be the uplink and downlink channel capacity of node $i$ at time slot $t$, respectively, given that channel $s$ is assigned to node $i$ and the full-duplex mode is selected. Assuming block fading channels, we have

$$C_i^u(t)|_{\alpha_i(t)=s,\beta_i(t)=F} = B\log_2\left(1 + \frac{p_i^u(t)\left|h_s^u\right|^2}{N_0 + p_i^d\eta_d}\right) \tag{3}$$

$$C_i^d(t)|_{\alpha_i(t)=s,\beta_i(t)=F} = B\log_2\left(1 + \frac{p_i^d(t)\left|h_s^d\right|^2}{N_0 + p_i^u\eta_u}\right) \tag{4}$$

where $B$ is the channel bandwidth; $h_s^u$ and $h_s^d$ are the channel gains between the AP and node $i$ for the uplink and downlink channel, respectively; $p_i^u(t) > 0$ and $p_i^d(t) > 0$ are the uplink and downlink transmit power, respectively; $\eta_d$ and $\eta_u$ are the self-interference cancellation ratio at the AP and node $i$, respectively; and $N_0$ is additive white Gaussian noise power.

For half-duplex uplink transmissions, the uplink channel capacity for node $i$, given that it is assigned with channel $s$, can be written as

$$C_i^u(t)|_{\alpha_i(t)=s,\beta_i(t)=U} = B\log_2\left(1 + \frac{p_i^u(t)\left|h_s^u\right|^2}{N_0}\right). \tag{5}$$

In this case, we have $p_i^u(t) > 0$ and $p_i^d(t) = 0$. For half-duplex downlink transmission, the downlink channel capacity for node $i$, given that it is assigned with channel $s$, can be written as

$$C_i^d(t)|_{\alpha_i(t)=s,\beta_i(t)=D} = B\log_2\left(1 + \frac{p_i^d(t)\left|h_s^d\right|^2}{N_0}\right). \tag{6}$$

In this case, we have $p_i^u(t) = 0$ and $p_i^d(t) > 0$.

Following the Lindley's equation, the dynamics of the uplink and downlink traffic queues can be described as

$$Q_i^u(t+1) = \max\left\{Q_i^u(t) + A_i^u(t) - B_i^u(t), 0\right\} \tag{7}$$

$$Q_i^d(t+1) = \max\left\{Q_i^d(t) + A_i^d(t) - B_i^d(t), 0\right\} \tag{8}$$

where $B_i^u(t) = (T/L)C_i^u(t)|_{\alpha_i(t),\ \beta_i(t)}$ and $B_i^d(t) = (T/L)C_i^d(t)|_{\alpha_i(t),\ \beta_i(t)}$ are the service rates in packets per time slot at time $t$ for the uplink and downlink queues, respectively; $T$ is the duration of a time slot, and $L$ is the packet length in bits.

### B. Problem Formulation

As can be seen from (3)–(6), the overall throughput can be enhanced with full-duplex transmissions, but at the cost of higher energy consumption. The energy efficiency maybe degraded due to the residual self-interference. There is a trade-off between the overall queue length (which is indicative of delay) and energy efficiency with different transmission mode selections. Although both energy efficiency and throughput can be enhanced by transmitting only on good channels, there may be the extra delay to wait for the channel condition to recover from a deep fade.

The average total energy consumption of the system, over both uplink and downlink, all nodes, and time slots, can be written as

$$\bar{P} \triangleq \limsup_{\Gamma\to\infty} \frac{1}{\Gamma}\sum_{t=0}^{\Gamma-1}\sum_{i=1}^{N}\mathbb{E}\left\{p_i^u(t) + p_i^d(t)\middle|\alpha_i(t), \beta_i(t)\right\}. \tag{9}$$

We also define the average queue length as

$$\bar{Q} \triangleq \limsup_{\Gamma\to\infty} \frac{1}{\Gamma}\sum_{t=0}^{\Gamma-1}\sum_{i=1}^{N}\mathbb{E}\left\{Q_i^u(t) + Q_i^d(t)\right\}. \tag{10}$$

We schedule the uplink and downlink transmissions at the beginning of each time slot. According to the notion of *throughput-optimal* [15], the objective is to minimize the average energy consumption while keeping all the uplink and downlink queues stable, when the input rates are within the system's capacity region. We have the following problem formulation:

$$\min: \quad \bar{P} = \limsup_{\Gamma\to\infty} \frac{1}{\Gamma}\sum_{t=0}^{\Gamma-1}\sum_{i=1}^{N}\mathbb{E}\left\{p_i^u(t) + p_i^d(t)\middle|\alpha_i(t), \beta_i(t)\right\} \tag{11}$$

$$\text{s.t.} \quad \alpha_i(t) \neq \alpha_j(t), \text{ if } \alpha_i(t) \in \mathcal{S} \text{ or } \alpha_j(t) \in \mathcal{S} \text{ for all } i \neq j, i, j \in \mathcal{N} \tag{12}$$

$$\bar{Q} < \infty, \text{ for all } \left\{\vec{\lambda}^u, \vec{\lambda}^d\right\} \in \vec{\Lambda} \tag{13}$$

where $\vec{\Lambda}$ is the capacity region of the WLAN system. Constraint (12) forbids two nodes accessing the same channel

and constraint (13) ensures that the schedule meets the notion of throughput-optimal.

## IV. Capacity Region and Throughput-Optimal Scheduling

As defined in [15] and [43], a system is considered stable under a scheduling policy $\Psi$ if the expectation of the queues lengths are bounded for an arrival rate vector $\vec{\lambda}$. The capacity region of a system is the set of all the arrival vectors under which the system can be stabilized with some scheduling policy. In other words, if an arrival rate vector is within the capacity region, then there exist a scheduling policy that can stabilize the system. Otherwise, the system cannot be stabilized by any scheduling policy if the arrival rate vector is outside the capacity region. We also define throughput-optimal scheduling based on the notation of capacity region as in [15]. A scheduling policy is throughput-optimal if it stabilizes the system under any arrival rate vector that is strictly within the capacity region.

### A. Capacity Region of the Multichannel Full-Duplex WLAN

We defined the capacity region of the system as follows. For any constant $\epsilon \geq 0$, if there is some scheduling policy that ensures

$$\lambda_i^u = \mathbb{E}\left\{A_i^u(t)\right\} \leq \mathbb{E}\left\{B_i^u(t)\right\} - \epsilon, \ i \in \mathcal{N} \tag{14}$$

$$\lambda_i^d = \mathbb{E}\left\{A_i^d(t)\right\} \leq \mathbb{E}\left\{B_i^d(t)\right\} - \epsilon, \ i \in \mathcal{N} \tag{15}$$

then $\vec{\lambda} = \{\vec{\lambda}^u, \vec{\lambda}^d\}$ is within the capacity region. All such $\vec{\lambda}$ vectors form the stability region of the multichannel full-duplex WLAN system.

The definition is straightforward. For given $\{\vec{\lambda}^u, \vec{\lambda}^d\}$ within the capacity region, if there exists some scheduling policy that ensures (14) and (15) for some $\epsilon \geq 0$, then such scheduling policy can stabilize the WLAN system.

### B. Capacity Region for Half-Duplex and Full-Duplex Systems

It is easy to see that the capacity region of a full-duplex system will be a super set of that of the corresponding half-duplex system. We use a special case to illustrate how the capacity region is expanded with full-duplex transmissions. Let us consider a system where $N = 1$ and $S = 1$ with fixed power $p_i^u(t) = p_i^u$ and $p_i^d(t) = p_i^d$. We also assume that the channel condition remains unchanged during the entire process. The we have the following properties for the capacity regions of full-duplex and half-duplex systems. The proofs are provided in Appendices A and B, respectively.

*Theorem 1:* For a half-duplex system with $N = 1$ and $S = 1$, the capacity region can be represented as follows:

$$\lambda_1^u/a + \lambda_1^d/b \leq 1 \tag{16}$$

where $a = \mathbb{E}\{(\mathrm{BT}/L)C_1^u|_{\alpha=1,\beta=U}\}$ and $b = \mathbb{E}\{(\mathrm{BT}/L)C_1^d|_{\alpha=1,\beta=D}\}$.

*Theorem 2:* Consider a full-duplex enabled system with $N = 1$ and $S = 1$. Define $\mu_a = C_1^u|_{\alpha=1,\beta=F}/C_1^u|_{\alpha=1,\beta=U}$ and $\mu_b = C_1^d|_{\alpha=1,\beta=F}/C_1^d|_{\alpha=1,\beta=D}$, where $C_1^u|_{\alpha=1,\beta=F}$, $C_1^d|_{\alpha=1,\beta=F}$, $C_1^u|_{\alpha=1,\beta=U}$, and $C_1^d|_{\alpha=1,\beta=D}$ are defined in (3)–(6), respectively. Recall that $a = \mathbb{E}\{(\mathrm{BT}/L)C_1^u|_{\alpha=1,\beta=U}\}$ and $b = \mathbb{E}\{(\mathrm{BT}/L)C_1^d|_{\alpha=1,\beta=D}\}$. The capacity region of this system can be presented as follows.

1) If $\mu_a + \mu_b \leq 1$, then the capacity region is degraded to that of the corresponding half-duplex system.
2) If $\mu_a + \mu_b > 1$, then

$$\lambda_1^u(1-\mu_b)/a + \lambda_1^d\mu_a/b \leq \mu_a, \ \text{if } \lambda_1^u/\lambda_1^d \geq \frac{a\mu_a}{b\mu_b} \tag{17}$$

$$\lambda_1^d l(1-\mu_a)/b + \lambda_1^u\mu_b/a \leq \mu_b, \ \text{otherwise.} \tag{18}$$

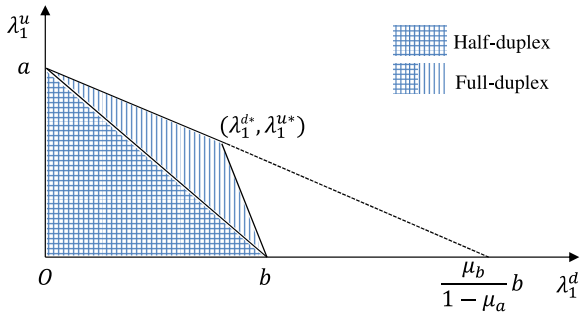


Fig. 2. Capacity region of a system with $N = 1$ and $S = 1$, when $\mu_a + \mu_b > 1$.

The capacity region when $\mu_a + \mu_b > 1$ is illustrated in Fig. 2. When $\mu_a + \mu_b \leq 1$, the capacity region of the full-duplex system is degraded to that of the corresponding half-duplex system (i.e., the triangle area). When $\mu_a + \mu_b > 1$, the capacity region of the full-duplex system is the expanded quadrilateral. The piece-wise linear boundary is defined by (17) and (18). It can be derived from (18) that when $\lambda_1^U = 0$, $\lambda_1^d = (\mu_b/1-\mu_a) \cdot b$, which is greater than $b$ since $\mu_a + \mu_b \leq 1$. Therefore the full-duplex capacity region is really larger than that of the half-duplex system. The vertex $(\lambda_1^{d*}, \lambda_1^{u*})$ is where the two lines defined by (17) and (18) intersect, as

$$\begin{cases} \lambda_1^{d*} = \frac{ab^2\mu_b(1-\mu_b)}{b^2\mu_b(1-\mu_b)-a^2\mu_a(1-\mu_a)} \\ \lambda_1^{u*} = \frac{a^2b\mu_a\mu_b}{a^2\mu_a(1-\mu_a)-b^2\mu_b(1-\mu_b)}. \end{cases} \tag{19}$$

## V. Solution Algorithm and Performance Analysis

In this section, we present a scheduling algorithm based on the Lyapunov optimization framework [17], which involves channel assignment [44], transmission schedule, and transmission mode selection for the multichannel full-duplex WLAN. The operation of this algorithm requires no stationary distribution or future information about the channel processes or the arrival processes to the queues. It only requires information on current uplink and downlink queue lengths and channel conditions, and is thus an *online* algorithm.

### A. Lyapunov Optimization-Based Scheduling Algorithm

Following the Lyapunov optimization framework, we first define the Lyapunov function $L(Q(t))$ as:

$$L(Q(t)) \triangleq \frac{1}{2}\sum_{i=1}^{N}\left\{\left\{Q_i^u(t)\right\}^2 + \left\{Q_i^d(t)\right\}^2\right\} \tag{20}$$

where $L(Q(0)) = 0$. Note that $L(Q(t))$ is small if and only if all the queue lengths are small; $L(Q(t))$ will become large if any of the queues is congested. The system is thus stable when $\mathbb{E}\{L(Q(t))\} < \infty$.

We then define the drift $\Delta(L(t))$ as

$$\Delta(L(t)) \triangleq \mathbb{E}\{L(Q(t+1)) - L(Q(t))|Q(t)\}. \tag{21}$$

Assuming $Q_i^u(0) = 0$ and $Q_i^d(0) = 0$, for all $i$, the system is stable when

$$\begin{aligned}\mathbb{E}\{L(Q(t))\} &= \mathbb{E}\left\{\sum_{k=0}^{t-1}[L(Q(k+1)) - L(Q(k))]\right\} \\ &= \sum_{k=0}^{t-1}\mathbb{E}\{L(Q(k+1)) - L(Q(k))|Q(k)\} \\ &= \sum_{k=0}^{t-1}\Delta(L(k)) < \infty. \end{aligned}\tag{22}$$

We can thus minimize the drift in every time slot $t$ to maintain a finite expectation for $L(Q(t))$.

It follows the queue dynamics (7) and (8) that:

$$\begin{aligned}&\left\{Q_i^u(t+1)\right\}^2 + \left\{Q_i^d(t+1)\right\}^2 \\ &\le \left\{Q_i^u(t) + A_i^u(t) - B_i^u(t)\right\}^2 + \left\{Q_i^d(t) + A_i^d(t) - B_i^d(t)\right\}^2 \\ &= \left\{Q_i^u(t)\right\}^2 + \left\{A_i^u(t) - B_i^u(t)\right\}^2 + 2Q_i^u(t)\left(A_i^u(t) - B_i^u(t)\right) \\ &\quad + \left\{Q_i^d(t)\right\}^2 + \left\{A_i^d(t) - B_i^d(t)r\right\}^2 + 2Q_i^d(t)\left(A_i^d(t) - B_i^d(t)\right).\end{aligned}\tag{23}$$

Substituting (23) into (21), we have

$$\begin{aligned}\Delta(L(t)) \le \Phi + \mathbb{E}\Bigg\{\sum_{i=1}^{N}\Big\{&Q_i^u(t)\left(A_i^u(t) - B_i^u(t)\right) \\ &+ Q_i^d(t)\left(A_i^d(t) - B_i^d(t)\right)\Big\}\Bigg\}\end{aligned}\tag{24}$$

where

$$\Phi = \frac{1}{2}\mathbb{E}\left\{\sum_{i=1}^{N}\left\{\left[A_i^u(t) - B_i^u(t)\right]^2 + \left[A_i^d(t) - B_i^d(t)\right]^2\right\}\right\} \tag{25}$$

which is bounded if the arrival rate and service rate of each uplink and downlink queue are bounded. This is true if the arrival rates are within the capacity region of the system.

Defining $P(t) \triangleq \sum_{i=1}^{N}\{p_i^u(t) + p_i^d(t)\}$, we then obtain the *drift-plus-penalty* $\Delta(L(t)) + V\mathbb{E}\{P(t)\}$ as in [17], by incorporating the energy penalty (i.e., the overall energy consumption at time $t$) with a positive coefficient $V$. Parameter $V$ indicates the significance of energy consumption to the nodes. That is, the more emphasis on energy consumption, the greater the value of $V$. In particular, $V = 0$ indicates that the nodes are not sensitive to energy consumption at all. Based on (24), we can derive an upper bound on the drift-plus-penalty as

$$\begin{aligned}&\Delta(L(t)) + V\mathbb{E}l\{P(t)\} \le \Phi + \mathbb{E}\{VP(t)\} \\ &+ \mathbb{E}\left\{\sum_{i=1}^{N}\left\{Q_i^u(t)\left(A_i^u(t) - B_i^u(t)\right) + Q_i^d(t)\left(A_i^d(t) - B_i^d(t)\right)\right\}\right\}.\end{aligned}\tag{26}$$

Ignoring the constant $\Phi$, we minimize the second and third terms on the right-hand-side of (26), that is

$$\begin{aligned}\Theta \triangleq VP(t) + \sum_{i=1}^{N}\Big\{&Q_i^u(t)\left(A_i^u(t) - B_i^u(t)\right) \\ &+ Q_i^d(t)\left(A_i^d(t) - B_i^d(t)r\right)\Big\}\end{aligned}\tag{27}$$

at each time slot $t$ in order to minimize the drift-plus-penalty. Notice that $\Theta$ can be rewritten as

$$\begin{aligned}\Theta = &\sum_{i=1}^{N}\left\{Q_i^u(t)A_i^u(t) + Q_i^d(t)A_i^d(t)\right\} \\ &- \sum_{i=1}^{N}\left\{Q_i^u(t)B_i^u(t) - Vp_i^u(t) + Q_i^d(t)B_i^d(t) - Vp_i^d(t)\right\}.\end{aligned}\tag{28}$$

The first term on the right-hand-side of (28), $\sum_{i=1}^{N}\{Q_i^u(t)A_i^u(t) + Q_i^d(t)A_i^d(t)\}$, only depends on the arrival rates and the current queue lengths. Therefore, it does not affect the scheduling decision. We only need to maximize (due to the negative sign) the second term of $\Theta$, which is a function of both $\alpha_i(t)$ and $\beta_i(t)$.

Let the channel assignment be $\vec{\alpha}(t) = \{\alpha_1(t), \alpha_2(t), \ldots, \alpha_N(t)\}$ and the transmission mode selection be $\vec{\beta}(t) = \{\beta_1(t), \beta_2(t), \ldots, \beta_N(t)\}$. We have

$$\begin{aligned}\Psi(t)\Big|_{\vec{\alpha}(t),\vec{\beta}(t)} &\triangleq \sum_{i=1}^{N}\Big\{Q_i^u(t)B_i^u(t) - Vp_i^u(t) \\ &\quad + Q_i^d(t)B_i^d(t) - Vp_i^d(t)\Big\}\Big|_{\alpha_i(t),\beta_i(t)} \\ &= \sum_{i=1}^{N}\psi_i(t)|_{\alpha_i(t),\beta_i(t)}\end{aligned}\tag{29}$$

where

$$\begin{aligned}\psi_i(t)\big|_{\alpha_i(t),\beta_i(t)} = \Big\{&Q_i^u(t)B_i^u(t) - Vp_i^u(t) + Q_i^d(t)B_i^d(t) \\ &- Vp_i^d(t)\Big\}\Big|_{\alpha_i(t),\beta_i(t)}.\end{aligned}\tag{30}$$

Let the optimal channel assignment be $\vec{\alpha}^*(t) = \{\alpha_1^*(t), \alpha_2^*(t), \ldots, \alpha_N^*(t)\}$ and the optimal transmission mode selection be $\vec{\beta}^*(t) = \{\beta_1^*(t), \beta_2^*(t), \ldots, \beta_N^*(t)\}$. To find the optimal schedule $\{\vec{\alpha}^*(t), \vec{\beta}^*(t)\}$, we first need to identify the transmission mode for a given channel assignment $\alpha_i(t) = s$ for each node $i$. That is

$$\beta_i^*(t)|_{\alpha_i(t)=s} = \underset{\beta_i(t)\in\{U,D,F\}}{\arg\max}\left\{\psi_i(t)|_{\alpha_i(t)=s,\beta_i(t)}\right\}. \tag{31}$$

Note that $\psi_i(t) = 0$ if no transmission is conducted. Therefore, we have

$$\psi_i^*(t)|_{\alpha_i(t)=s} = \max\left\{\psi_i(t)|_{\alpha_i(t)=s,\beta_i^*(t)}, 0\right\} \tag{32}$$

$$\vec{\psi}_i^*(t)|_{\alpha_i(t)} \triangleq \left\{\psi_i^*(t)|_{\alpha_i(t)=1}, \psi_i^*(t)|_{\alpha_i(t)=2}, \ldots, \psi_i^*(t)|_{\alpha_i(t)=S}\right\}. \tag{33}$$

We need to find the optimal channel assignment $\vec{\alpha}^*(t)$ based on $\vec{\psi}_i^*(t)|_{\alpha_i(t)}$, for $i = 1, 2, \ldots, N$. The channel assignment

**Algorithm 1:** Scheduling Algorithm for Channel Assignment and Transmission Mode Selection

1 Update all uplink and downlink queues and estimate all channel conditions at the beginning of each time slot $t$ ;
2 For each node $i$, find the transmission mode $\beta_i^*(t)|_{\alpha_i(t)=s}$ as in (31) ;
3 Obtain the channel assignment matrix $\{\vec{\psi}_1^*(t)|_{\alpha_1(t)}^T, \vec{\psi}_2^*(t)|_{\alpha_2(t)}^T, \ldots, \vec{\psi}_N^*(t)|_{\alpha_N(t)}^T\}$ ;
4 Apply the Hungarian method and (31) to find the optimal schedule $\{\vec{\alpha}^*(t), \vec{\beta}^*(t)\}$ ;
5 **if** $\psi_i(t)|_{\{\alpha_i^*(t),\beta_i^*(t)\}} > 0$ **then**
6 node $i$ transmits on channel $\alpha_i^*(t)$ with transmission mode $\beta_i^*(t)$;
7 **end**

problem can be transformed into a *maximum weighted bipartite matching problem* [42]. In the bipartite graph $\mathcal{G}$, nodes and the channels represent the two independent sets of vertices: 1) the set of nodes $G_1$ and 2) the set of channels $G_2$. In graph $\mathcal{G}$, the weight of the edge between a vertex in $G_1$ (i.e., a node $i$) and another vertex in $G_2$ (i.e., a channel $s$) is set to $\psi_i^*(t)|_{\alpha_i(t)=s}$. This way, the maximum weighted bipartite matching of graph $\mathcal{G}$ corresponds to the optimal channel assignment $\vec{\alpha}^*(t)$. The maximum weighted bipartite matching problem can be solved with the Hungarian method [18]. The complexity of the Hungarian method is $O(NS^2)$ if $N > S$, or $O(N^2S)$ if $N \leq S$.

When the optimal channel assignment is solved, the optimal transmission mode $\beta_i^*(t)$ for node $i$ is readily obtained as in (31), i.e., $\beta_i^*(t) = \beta_i^*(t)|_{\alpha_i^*(t)}$. Now we obtain the optimal schedule $\{\vec{\alpha}^*(t), \vec{\beta}^*(t)\}$ as well as the corresponding $\Psi(t)|_{\vec{\alpha}^*(t),\vec{\beta}^*(t)}$. Then we can assign the channels and decide the transmission mode for each node based on the optimal schedule. Note that $\psi_i(t)|_{\alpha_i^*(t),\beta_i^*(t)} = 0$ if no transmission is scheduled for node $i$; so node $i$ transmits if and only if $\psi_i(t)|_{\alpha_i^*(t),\beta_i^*(t)} > 0$.

The detailed algorithm for deriving the optimum schedule $\{\vec{\alpha}^*(t), \vec{\beta}^*(t)\}$ is presented in Algorithm 1, which is executed at the beginning of each time slot.

### B. Performance Analysis

We have the following theorem on the optimality of Algorithm 1.

*Theorem 3:* The schedule $\{\vec{\alpha}^*(t), \vec{\beta}^*(t)\}$ obtained by Algorithm 1 achieves the maximum $\Psi(t)$.

*Proof:* For any schedule $\{\vec{\alpha}(t), \vec{\beta}(t)\}$, we have $\Psi(t)|_{\vec{\alpha}(t),\vec{\beta}(t)} \leq \Psi(t)|_{\vec{\alpha}(t),\vec{\beta}^*(t)}$, where $\vec{\beta}^*(t)$ is the transmission mode selection under channel assignment $\vec{\alpha}(t)$ as in (31). We also have $\Psi(t)|_{\vec{\alpha}(t),\vec{\beta}^*(t)} \leq \Psi(t)|_{\vec{\alpha}*(t),\vec{\beta}^*(t)}$ for any channel assignment $\vec{\alpha}(t)$, according to maximum weighted bipartite matching. Therefore schedule $\{\vec{\alpha}^*(t), \vec{\beta}^*(t)\}$ is optimal.

We also derive the upper bounds for the expectations of average sum queue lengths of all the uplink and downlink queues and the corresponding average total energy consumption as follows. The proof is provided in Appendix C.

*Theorem 4:* Assume that the arrival rates to the queues, $\vec{\lambda}^u$ and $\vec{\lambda}^d$, are strictly within the system's capacity region, i.e., the system can be stabilized under certain $\{\vec{\alpha}(t), \vec{\beta}(t)\}$. Then the upper bounds on the average sum queue lengths and average energy consumption under Algorithm 1 can be derived as

$$\limsup_{\Gamma\to\infty} \frac{1}{\Gamma} \sum_{t=1}^{\Gamma-1} \sum_{i=1}^{N} \mathbb{E}\{Q_i^u(t) + Q_i^d(t)\} \leq \frac{1}{\epsilon}(\Phi + VP) \quad (34)$$

$$\limsup_{\Gamma\to\infty} \frac{1}{\Gamma} \sum_{t=1}^{\Gamma-1} \sum_{i=1}^{N} \mathbb{E}\left\{p_i^u(t) + p_i^d(t)\right\} \leq P^{\text{opt}} + \frac{\Phi}{V} \quad (35)$$

where $P^{\text{opt}}$ is the minimum average energy consumption under any stable scheduling strategy, $P$ is the average energy consumption under the proposed algorithm, $\epsilon > 0$ is the distance between the arrival rates $\{\vec{\lambda}^u, \vec{\lambda}^d\}$ and the system capacity region under the proposed algorithm, and $\Phi$ is given in (24).

The asymptotic stability performance of Algorithm 1 is given in the following theorem. The proof is provided in Appendix D.

*Theorem 5:* If the arrival rate vector $\{\vec{\lambda}^u, \vec{\lambda}^d\}$ is in the capacity region, $\mathbb{E}\{A_i^u(t)\}^2 \leq D$ and $\mathbb{E}\{A_i^d(t)\}^2 \leq D$ for all $i \in \mathcal{N}$. Then under Algorithm 1, we have

$$\lim_{t\to\infty} \frac{Q(t)}{t} = 0 \quad (36)$$

where $Q(t) = \left\{Q_i^u(t), Q_i^d(t)\right\}$ for all $i \in \mathcal{N}$.

## VI. Performance Evaluation

In this section, we evaluate the performance of the proposed algorithm through MATLAB simulations. We assume that the maximum transmit power is 46 dBm at the AP and 23 dBm at the nodes. We assume a 110 dB self-interference cancellation in both uplink and downlink transceivers. For the wireless channels, we adopt the commonly used Okumura-Hata model for small and medium-sized cities. Each channel has a bandwidth of 360 kHz. There are 12 nodes and 10 channels in the WLAN system.

We compare the average energy consumptions and queue lengths of a half-duplex only system and a full-duplex system under different $V$ values. The simulation results are presented in Figs. 3–6 for different traffic arrival rates. From the simulations, we find that the full-duplex system always outperforms the half-duplex only system with respect to both average queue length and energy consumption. Moreover, there is a tradeoff between the average queue length and energy consumption for the full-duplex system under different $V$ values.

We also validate the capacity region analysis for both half-duplex only system and full-duplex system. The simulated results are presented in Figs. 7–9. For the one channel and one node system, the simulations confirm the shape of the expanded capacity region of the full-duplex system, as indicated by our analysis. We also find that for multiple-channel systems, the full-duplex capacity region also expands in similar manner as in the one channel and one node system.

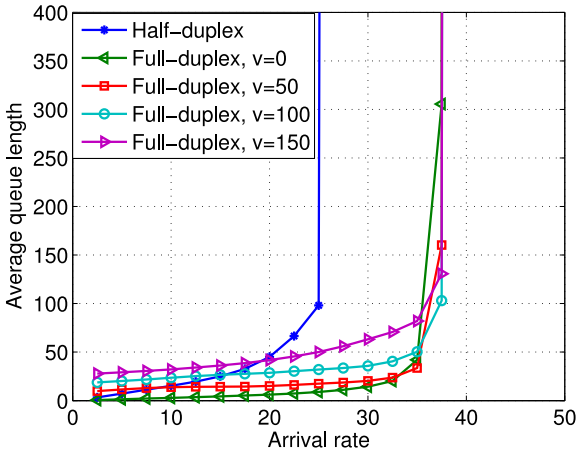


Fig. 3. Average queue lengths achieved by the proposed algorithm.

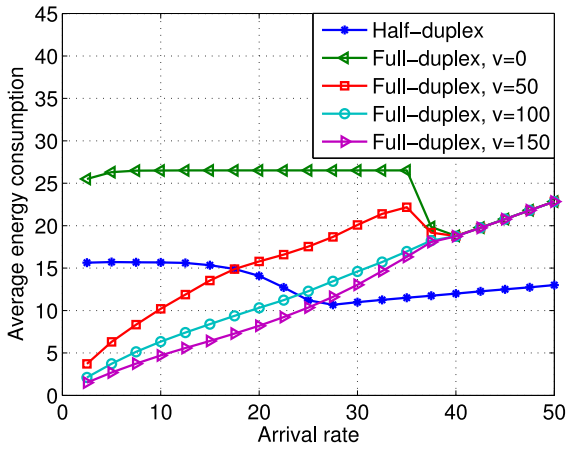


Fig. 4. Average energy consumptions achieved by the proposed algorithm.

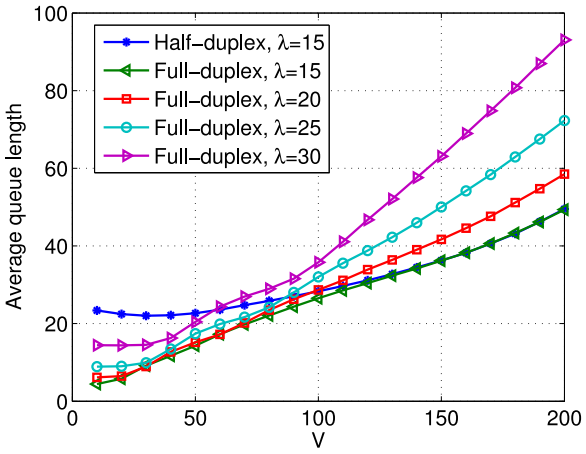


Fig. 5. Average queue lengths achieved by the proposed algorithm.

More specifically, Fig. 3 presents the average queue length versus traffic load. When $V = 0$, the scheme only minimizes the drift and does not care about energy consumption. In this case, the average queue length of the half-duplex case is always greater than that of the full-duplex case. Moreover, in the half-duplex only case, the queues cannot be stabilized when the arrival rate exceeds 25. In the full-duplex case, the queues can be stabilized until the arrival rate reaches 38. Clearly, full-duplex transmissions are helpful to keep the queue backlog low and increase the capacity region of the WLAN. It is also interesting to see that for all the full-duplex cases, the queues can be stabilized when the arrival rate is lower than 38, indicating that different $V$ values do not affect the stability of the system. Moreover, the average queue length increases when $V$ is increased, as indicated by the upper bound of average queue length (34) in Theorem 4.

Fig. 4 presents the average energy consumption versus traffic load. We find the average energy consumption of the half-duplex only case is smaller than that of the full-duplex cases under heavy load, when the queues become unstable. However, in the stable capacity region of the half-duplex only case (i.e., when the arrival rate is lower than 25), the average energy consumption of the half-duplex only case is greater than that of the full-duplex cases with $V > 50$. This is because when $V > 50$, the energy consumption is more seriously considered (i.e., in the drift-plus-penalty) and the nodes would transmit only when the energy efficiency is high. For the full-duplex case with $V = 0$, the average energy consumption is the highest among all the cases, since the proposed scheme does not consider energy efficiency. Furthermore, the energy consumption drops when the arrival rate is greater than 38. This is due to the unbalanced service rates of the uplink and downlink. When the queues are not stable, more uplink transmissions were made; the uplink transmit power is comparatively smaller than that of the downlink transmissions. Finally, it can be seen that the energy consumption decreases when $V$ is increased, as indicated by the upper bound of average energy consumption (35) in Theorem 4.

Fig. 5 presents the average queue length versus $V$ values. It shows that the average queue length increases almost linearly with $V$, which conforms the analysis in (34). With a small $V$ value, i.e., $V < 125$, the average queue length of the full-duplex system is shorter than that of the half-duplex only system. It indicates that when power consumption is not a concern, full-duplex has been used to reduce the queue length. With a high $V$ value, the queue length curve of the full-duplex system almost overlaps with that of the half-duplex system. It indicates that when power consumption becomes an issue, full-duplex transmission is rarely applied.

Fig. 6 presents the average energy consumption versus $V$ values. It shows that the average power consumption decreases as $V$ is increased, which validates the analysis in (35). With a small $V$ value, i.e., $V < 125$, the full-duplex system consumes more power by invoking full-duplex transmissions to reduce the queue length. With a high $V$ value, full-duplex transmission is rarely used and the power consumption of the full-duplex system is almost the same as that of the half-duplex system (when $\lambda = 15$ in both cases).

We next present our simulation results on capacity region. In Fig. 7, we plot the capacity region of a one node and one channel system. We show the average queue length versus downlink arrival rate $\lambda_1^d$, while the uplink arrival rate $\lambda_1^u$ is fixed at different values. When the queue length goes to infinity, the corresponding downlink arrival rate $\lambda_1^d$ indicates the maximum

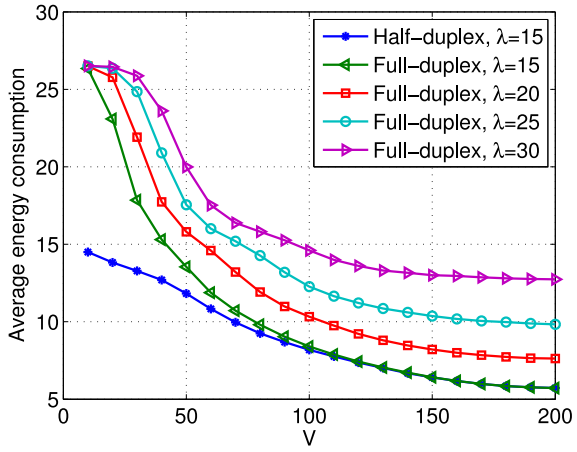


Fig. 6. Average energy consumptions achieved by the proposed algorithm.

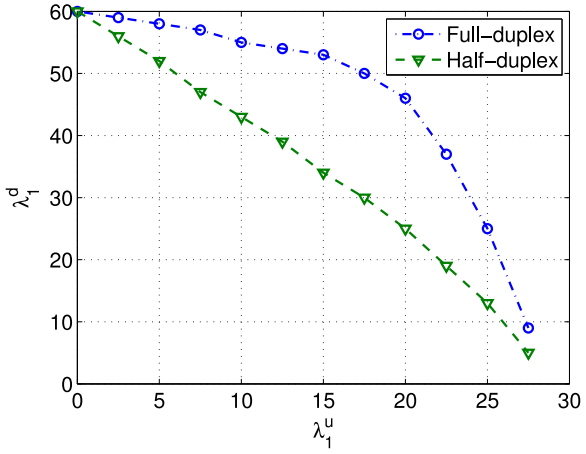


Fig. 8. Capacity region of the one-channel/one-node system.

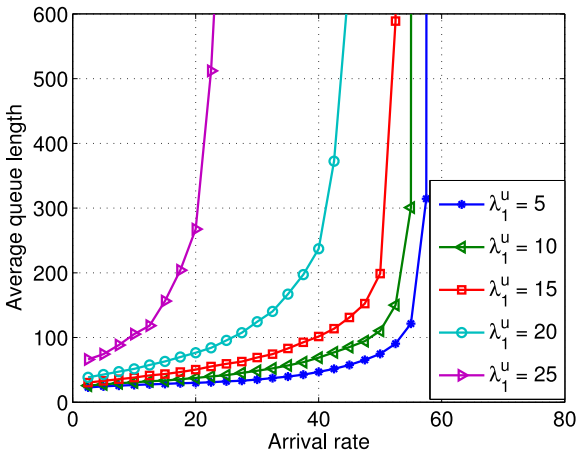


Fig. 7. Average queue lengths versus downlink arrival rate with one channel and one node.

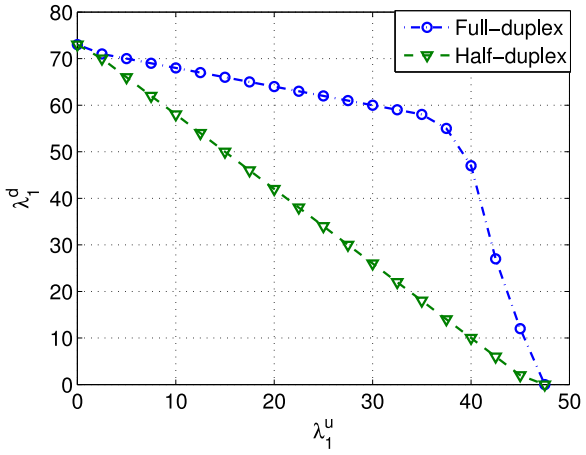


Fig. 9. Capacity region of the 10-channel/12-node system.

capacity the system can provide. It can be seen that the maximum downlink arrival rate decreases as the maximum uplink arrival rate is increased. We find that for $\lambda_1^u = 5,\ 10,\ 15$, the decreasing rate of the maximum $\lambda_1^d$ is much smaller than that for $\lambda_1^u = 20,\ 25$. This is because the capacity region is expanded when full-duplex transmissions are enabled.

The capacity regions for full-duplex and half-duplex systems are presented in Figs. 8 and 9, for the one node/one channel system and a 12-node/10-channel system, respectively. It can be seen that the capacity region of the half-duplex system is in the form of a triangle. The capacity region of the full-duplex system is in the form of a quadrilateral, which encompasses the capacity region of the half-duplex system. When $\lambda_1^u = 0$, both half-duplex and full-duplex systems have the same capacity (i.e., $b$ in Fig. 2), as full-duplex cannot be applied when there is no bidirectional traffic. This simulation study also verifies the capacity region analysis presented in Section IV-A. We also notice that the capacity region for the 12-node/10-channel system has a similar form, but is larger than that of the one-node/one-channel system. This is due to the channel diversity in the multichannel system.

## VII. Conclusion

In this paper, we proposed a scheduling algorithm to jointly decide the channel assignment, transmission scheduling, half- or full-duplex transmission mode selection for each node in a multichannel full-duplex WLAN. The proposed scheme was based on Lyapunov optimization and is an online algorithm. We also proved the optimality of the proposed algorithm and derived upper bounds for the average queue length and energy consumption under the proposed algorithm. We evaluated the performance of the proposed algorithm with simulations. We showed that under the proposed algorithm, there was a tradeoff between the average queue length and energy consumption with different $V$ values.

## Appendix A
## Proof for Theorem 1

We examine two cases. The first case is when $\lambda_1^u/a + \lambda_1^d/b \leq 1$. Consider a scheduling policy that schedules half-duplex uplink transmission with probability $\pi_1^u = (\lambda_1^u/a/\lambda_1^u/a + \lambda_1^d/b)$ and half-duplex downlink transmission with probability $\pi_1^d = (\lambda_1^d/b/\lambda_1^u/a + \lambda_1^d/b)$. Then following (5) and (6), we have $\mathbb{E}\{B_1^u\} = (\lambda_1^u/\lambda_1^u/a + \lambda_1^d/b)$ and

$\mathbb{E}\{B_1^d\} = (\lambda_1^d/\lambda_1^u/a + \lambda_1^d/b)$. Let $\delta = 1/\{\lambda_1^u/a + \lambda_1^d/b\} - 1$. We have

$$\mathbb{E}\left\{B_1^u\right\} = \lambda_1^u + \lambda_1^d\delta, \quad \mathbb{E}\left\{B_1^d\right\} = \lambda_1^d + \lambda_1^d\delta.$$

As $\lambda_1^u/a + \lambda_1^d/b \leq 1$, then we

$$\delta = 1/\left\{\mathbb{E}\left\{A_1^u\right\}/a + \mathbb{E}\left\{A_1^d\right\}/b\right\} - 1 \geq 0. \tag{37}$$

Then (14) and (15) hold.

When $\lambda_1^u/a + \lambda_1^d/b > 1$, constraints (14) and (15) require scheduling half-duplex uplink transmission with a probability at least $\lambda_1^u/a$ and scheduling half-duplex downlink transmission with a probability at least $\lambda_1^d/b$. Since $\lambda_1^u/a + \lambda_1^d/b > 1$, such a scheduling policy is invalid. Hence no scheduling policy can stabilize the system in this case.

## Appendix B
## Proof for Theorem 2

If $\mu_a + \mu_b \leq 1$, the system does not benefit from full-duplex transmissions. If a node uses full-duplex transmissions with a probability $\pi$, it achieves a throughput of $\pi a\mu_a$ for the uplink and $\pi b\mu_b$ for the downlink. To achieve the same throughput, it only needs to conduct half-duplex uplink transmissions with a probability $\pi\mu_a$ and half-duplex downlink transmissions with probability $\pi\mu_b$, whereas

$$\pi\mu_a + \pi\mu_b = \pi(\mu_a + \mu_b) \leq \pi. \tag{38}$$

So full-duplex transmissions do not increase throughput for the system. In this case, if the system can be stabilized by a schedule policy when full-duplex is enabled, it should be stabilized by a schedule policy with only half-duplex transmissions. Therefore, the capacity region of the full-duplex system is degraded to that of the corresponding half-duplex system in this case.

If $\mu_a + \mu_b > 1$, we derive the capacity region when $\lambda_1^u/\lambda_1^d \geq (a\mu_a/b\mu_b)$. For the case when $\lambda_1^u/\lambda_1^d < (a\mu_a/b\mu_b)$, the proof is similar and we omit it for brevity.

We first prove that the system can be stabilized with some scheduling policy if the arrival rate vector satisfies (17). If we schedule full-duplex transmissions with a probability $(\lambda_1^d/(b\mu_b)/\lambda_1^u(1-\mu_b)/(a\mu_a) + \lambda_1^d/b) \geq 0$, and half-duplex uplink transmissions with probability $(\lambda_1^u/a - \lambda^d\mu_a/(b\mu_b)/\lambda_1^u(1-\mu_b)/(a\mu_a) + \lambda_1^d/b) \geq 0$, then we have

$$\mathbb{E}\left\{B_1^d\right\} = \frac{\lambda_1^d/(b\mu_b)}{\lambda_1^u(1-\mu_b)/(a\mu_a) + \lambda_1^d/b} \times b\mu_b \geq \lambda_1^d$$

since $\lambda_1^u(1-\mu_b)/(a\mu_a) + \lambda_1^d/b \leq 1$. We also have

$$\mathbb{E}\left\{B_1^u\right\} = \frac{\left(\lambda_1^u/a - \lambda_1^d\mu_a/(b\mu_b)\right) \times a + \lambda_1^d/(b\mu_b) \times a\mu_a}{\lambda_1^u(1-\mu_b)/(a\mu_a) + \lambda_1^d/b} = \frac{\lambda_1^u}{\lambda_1^u(1-\mu_b)/(a\mu_a) + \lambda_1^d/b} \geq \lambda_1^u$$

since $\lambda_1^u(1-\mu_b)/(a\mu_a) + \lambda_1^d/b \leq 1$. Therefore the system can be stabilized with some scheduling policy.

Next, we prove that if the arrival rate vector is beyond the defined capacity region, that is,

$$\lambda_1^u(1-\mu_b)/a + \lambda_1^d\mu_a/b > \mu_a \tag{39}$$

then there is no scheduling policy that can stabilize the system. We also only prove the case of $\lambda_1^u/\lambda_1^d \geq (a\mu_a/b\mu_b)$, while the proof for the case $\lambda_1^u/\lambda_1^d < (a\mu_a/b\mu_b)$ is similar and omitted for brevity. For ease of presentation, we define the probability of half-duplex uplink transmission as $\pi_1^u$, the probability of half-duplex downlink transmission as $\pi_1^d$, and the probability of full-duplex transmission as $\pi_1^f$.

Assume a scheduling policy $\Psi$ with $\pi_1^d = 0$. To stabilize the system, the downlink throughput should be no less than the downlink arrival rate to the queue, that is,

$$\pi_1^f b\mu_b \geq \lambda_1^d. \tag{40}$$

Furthermore, the uplink throughput should be no less than the uplink arrival rate to the queue, that is,

$$\pi_1^u a + \pi_1^f a\mu_a \geq \lambda_1^u. \tag{41}$$

Substituting (40) and (41) into (39), we have

$$\pi_1^u(1-\mu_b)/\mu_a + \pi_1^f > 1. \tag{42}$$

Since $\mu_a + \mu_b > 1$, we have $(1-\mu_b)/\mu_a < 1$. Thus it follows (42) that:

$$\pi_1^u + \pi_1^f > 1.$$

So $\Psi$ is invalid and there is no schedule policy with $\pi_1^d = 0$ that can stabilize the system.

We next examine two cases and show the following.

1) $\pi_1^u/\pi_1^d > \mu_a/\mu_b$*:* If there is a feasible scheduling policy $\psi$ with $\pi_1^d > 0$ that can stabilize the system, then there is a corresponding scheduling policy $\psi'$ with $\pi_1'^d = 0$ that can also stabilize the system.
2) $\pi_1^u/\pi_1^d \leq \mu_a/\mu_b$*:* If there is a feasible scheduling policy $\psi$ with $\pi_1^u > 0$ that can stabilize the system, then we can derive a feasible scheduling policy $\psi'$ with $\pi_1'^u = 0$ that can also stabilize the system.

*Case I:* If $\pi_1^u/\pi_1^d > \mu_a/\mu_b$, then consider the following policy $\psi'$ with $\pi_1'^u = \pi_1^u - \pi_1^d \cdot (\mu_a/\mu_b)$, $\pi_1'^d = 0$, and $\pi_1'^f = \pi_1^f + \pi_1^d/\mu_b$. We have

$$\pi_1'^u + \pi_1'^d + \pi_1'^f = \pi_1^u + \pi_1^d \cdot \frac{1-\mu_a}{\mu_b} + \pi_1^f < \pi_1^u + \pi_1^d + \pi_1^f.$$

The inequality is due to $\mu_a + \mu_b > 1$. Thus $\psi'$ is feasible and can achieve a throughput no less than that of $\psi$. It can stabilize the system.

*Case II:* If $\pi_1^u/\pi_1^d \leq \mu_a/\mu_b$, then consider the following policy $\psi'$ with $\pi_1'^u = 0$, $\pi_1'^d = \pi_1^d - \pi_1^u \cdot (\mu_b/\mu_a)$, and $\pi_1'^f = \pi_1^f + \pi_1^u/\mu_a$. We can also show that

$$\pi_1'^u + \pi_1'^d + \pi_1'^f = \pi_1^u \cdot \frac{1-\mu_b}{\mu_a} + \pi_1^d + \pi_1^f < \pi_1^u + \pi_1^d + \pi_1^f.$$

Thus $\psi'$ is feasible and can stabilize the system.

Furthermore, since $\psi'$ stabilizes the system, the uplink throughput should be no less than the uplink arrival rate, i.e., $\pi_1'^u \cdot a + \pi_1'^f \cdot a\mu_a \geq \lambda_1^u$. Since $\pi_1'^u = 0$, we have

$$\pi_1'^f \geq \frac{\lambda_1^u}{a\mu_a}. \tag{43}$$

Substitute the inequality $\lambda_1^u/\lambda_1^d \geq (a\mu_a/b\mu_b)$ in to (43), we have

$$\pi_1'^f b\mu_b \geq \lambda_1^d. \tag{44}$$

That is, the throughput of full-duplex transmissions alone should stabilize the downlink queue. Hence we conclude that a schedule policy $\psi''$ with $\pi_1''^u = 0$, $\pi_1''^d = 0$, and $\pi_1''^f = \pi_1^f + \pi_1^u/\mu_a$ can stabilize the system.

## Appendix C
## Proof for Theorem 4

According to Theorem 3, Algorithm 1 maximizes $\Psi(t)$, which then minimizes $\Theta(t)$. It follows that:

$$\begin{aligned}\min\{\Theta(t)\} &= \min\left\{\sum_{i=1}^{N}\left\{Q_i^u(t)\left(A_i^u(t) - B_i^u(t)\right)\right.\right.\\ &\qquad \left.\left. + \; Q_i^d(t)(A_i^d(t) - B_i^d(t))\right\} + VP(t)\right\}\\ &\leq \sum_{i=1}^{N}\left\{Q_i^{u*}(t)\left(A_i^u(t) - B_i^{u*}(t)\right)\right.\\ &\qquad \left. + \; Q_i^{d*}(t)\left(A_i^d(t) - B_i^{d*}(t)\right)\right\} + VP^*(t)\end{aligned} \tag{45}$$

where $Q_i^{u*}$, $Q_i^{d*}$, $B_i^{d*}(t)$, and $P^*(t)$ are the terms corresponding to any (possible randomized) scheme. Now consider a randomized scheduling policy that achieves the optimal energy consumption and stabilizes the system, i.e., for $i \in \mathcal{N}$

$$\mathbb{E}\left\{P^*(t)\right\} = P^{\text{opt}} \tag{46}$$

$$\mathbb{E}\left\{A_i^u(t) - B_i^{u*}(t)\right\} \leq 0 \tag{47}$$

$$\mathbb{E}\left\{A_i^d(t) - B_i^{d*}(t)\right\} \leq 0 \tag{48}$$

where $P^{\text{opt}}$ is the minimal energy consumption under the corresponding scheduling policy that stabilizes the system, i.e., both (47) and (48) are satisfied.

Then with Algorithm 1, we have

$$\begin{aligned}\Delta(L(t)r) + V\mathbb{E}\{P(t)\} &\leq \Phi + \mathbb{E}\{\min\{\Theta(t)\}\}\\ &\leq \Phi + \mathbb{E}\left\{\sum_{i=1}^{N}\left\{Q_i^{u*}(t)\left(A_i^u(t) - B_i^{u*}(t)\right)\right\}\right\}\\ &\quad + \mathbb{E}\left\{\sum_{i=1}^{N}\left\{Q_i^{d*}(t)\left(A_i^d(t) - B_i^{d*}(t)\right)\right\}\right\} + V\mathbb{E}\left\{P^*(t)\right\}.\end{aligned} \tag{49}$$

As $Q_i^{u*}(t)$ is independent to $(A_i^u(t) - B_i^{u*}(t))$ and $Q_i^{d*}(t)$ is independent to $(A_i^d(t) - B_i^{d*}(t))$, along with (47) and (48), we have

$$\mathbb{E}\left\{Q_i^{u*}(t)\left(A_i^u(t) - B_i^{u*}(t)\right)\right\} \leq 0 \tag{50}$$

$$\mathbb{E}\left\{Q_i^{d*}(t)\left(A_i^d(t) - B_i^{d*}(t)\right)\right\} \leq 0 \tag{51}$$

for all $i \in \mathcal{N}$. Substituting (50) and (51) into (45), we have

$$\Delta(L(t)) + V\mathbb{E}\{P(t)\} \leq \Phi + 0 + V\mathbb{E}\left\{P^*(t)\right\} = \Phi + VP^{\text{opt}}.$$

For a stable system, we have $\sum_{t=0}^{T-1}\Delta(L(t)) = L(T) < \infty$. It follows that:

$$\begin{aligned}&\limsup_{T\to\infty}\frac{1}{T}\sum_{t=0}^{T-1}\Delta(L(t)) + \limsup_{T\to\infty}\frac{V}{T}\sum_{t=0}^{T-1}\mathbb{E}\{P(t)\}\\ &\quad = \limsup_{T\to\infty}\frac{V}{T}\sum_{t=0}^{T-1}\mathbb{E}\{P(t)\}\\ &\quad = \limsup_{T\to\infty}\frac{V}{T}\sum_{k=0}^{T-1}\mathbb{E}\left\{p_i^u(t) + p_i^d(t)\right\} \leq \Phi + V\cdot P^{\text{opt}}.\end{aligned} \tag{52}$$

Then (35) holds true.

Suppose that the system can be stabilized under the proposed scheduling algorithm and for all $i \in \mathcal{N}$ there exist a real number $\epsilon \geq 0$, such that

$$\mathbb{E}\left\{A_i^u(t) - B_i^u(t) \leq -\epsilon\right\} \tag{53}$$

$$\mathbb{E}\left\{A_i^d(t) - B_i^d(t) \leq -\epsilon\right\}. \tag{54}$$

Then we have

$$\begin{aligned}\Delta(L(t)) + V\mathbb{E}\{P(t)\} &\leq \Phi + \mathbb{E}\left\{\sum_{i=1}^{N}\left\{Q_i^u(t)\left(A_i^u(t) - B_i^u(t)\right)\right\}\right\}\\ &\quad + \mathbb{E}\left\{\sum_{i=1}^{N}\left\{Q_i^d(t)\left(A_i^d(t) - B_i^d(t)\right)\right\}\right\} + V\mathbb{E}\{P(t)\}\end{aligned} \tag{55}$$

$$\begin{aligned}&\leq \Phi - \mathbb{E}\left\{\sum_{i=1}^{N}\epsilon Q_i^u(t)\right\} - \mathbb{E}\left\{\sum_{i=1}^{N}\epsilon Q_i^d(t)\right\} + V\mathbb{E}\{P(t)\}\\ &= \Phi - \epsilon\mathbb{E}\left\{\sum_{i=1}^{N}\left\{Q_i^u(t) + Q_i^d(t)\right\}\right\} + V\mathbb{E}\{P(t)\}.\end{aligned} \tag{56}$$

Note that $\Delta(L(t)) + V\mathbb{E}\{P(t)\} \geq 0$ is guaranteed in Algorithm 1. Thus we have

$$\mathbb{E}\left\{\sum_{i=1}^{N}\left\{Q_i^u(t) + Q_i^d(t)\right\}\right\} \leq \frac{1}{\epsilon}\{\Phi + V\mathbb{E}\{P(t)\}\}. \tag{57}$$

It follows that:

$$\begin{aligned}&\limsup_{T\to\infty}\frac{1}{T}\sum_{t=1}^{T-1}\sum_{i=1}^{N}\mathbb{E}\left\{Q_i^u(t) + Q_i^d(t)\right\}\\ &\qquad \leq \frac{\Phi}{\epsilon} + \frac{1}{\epsilon}\limsup_{T\to\infty}\frac{1}{T}\{V\mathbb{E}\{P(t)\}\} = \frac{1}{\epsilon}(\Phi + VP).\end{aligned} \tag{58}$$

Then (34) holds true.

## Appendix D
## Proof for Theorem 5

According to Theorem 3, the schedule $\{\vec{\alpha}^*(t), \vec{\beta}^*(t)\}$ obtained by Algorithm 1 achieves the maximum $\Psi(t)$, i.e.,

the minimum bound on the drift-plus-drift

$$\begin{aligned}
&\Delta(L(t)) + V\mathbb{E}\{P(t)\} \\
&\le \Phi + \mathbb{E}\Bigg\{\min\Bigg\{\sum_{i=1}^{N}\Bigg\{Q_i^u(t)(A_i^u(t) - B_i^u(t)) \\
&\qquad + Q_i^d(t)\Big(A_i^d(t) - B_i^d(t)\Big)\Bigg\} + VP(t)\Bigg\}\Bigg\} \\
&\le \Phi + \mathbb{E}\Bigg\{\min\Bigg\{\sum_{i=1}^{N}\Bigg\{Q_i^u(t)\big(A_i^u(t) - B_i^u(t)\big) \\
&\qquad + Q_i^d(t)\Big(A_i^d(t) - B_i^d(t)\Big)\Bigg\}\Bigg\}\Bigg\} \\
&\quad + \mathbb{E}\{\min\{VP(t)\}\} \\
&\le \Phi + \mathbb{E}\Bigg\{\min\Bigg\{\sum_{i=1}^{N}\Bigg\{Q_i^u(t)\big(A_i^u(t) - B_i^u(t)\big) \\
&\qquad + Q_i^d(t)\Big(A_i^d(t) - B_i^d(t)\Big)\Bigg\}\Bigg\}\Bigg\} \\
&\quad + \max\{VP(t)\}
\end{aligned}$$

where $\max\{P(t)\}$ is maximum power consumption of the system, which is a bounded constant.

According to our definition of capacity region, there exists a feasible schedule policy $\Omega^*$ such that

$$\begin{aligned}
\mathbb{E}\Big\{A_i^{u*}(t) - B_i^{u*}(t)\Big\} < 0, \text{ for all } i \in \mathcal{N} \\
\mathbb{E}\Big\{A_i^{d*}(t) - B_i^{d*}(t)\Big\} < 0, \text{ for all } i \in \mathcal{N}
\end{aligned}$$

where $A_i^{u*}(t)$, $B_i^{u*}(t)$, $A_i^{d*}(t)$, and $B_i^{d*}(t)$ are arrivals and departures to the uplink and downlink traffic queues, respectively. Hence, the upper bound of the drift-plus-penalty can be rewritten as

$$\begin{aligned}
&\Delta(L(t)) + V\mathbb{E}\{P(t)\} \\
&\le \Phi + \mathbb{E}\Bigg\{\min\Bigg\{\sum_{i=1}^{N}\Bigg\{Q_i^u(t)\big(A_i^u(t) - B_i^u(t)\big) \\
&\qquad + Q_i^d(t)\Big(A_i^d(t) - B_i^d(t)\Big)\Bigg\}\Bigg\}\Bigg\} \\
&\quad + V\max\{P(t)\} \\
&\le \Phi + \mathbb{E}\Bigg\{\min\Bigg\{\sum_{i=1}^{N}\Bigg\{Q_i^u(t)\big(A_i^{u*}(t) - B_i^{u*}(t)\big) \\
&\qquad + Q_i^d(t)\Big(A_i^{d*}(t) - B_i^{d*}(t)\Big)\Bigg\}\Bigg\}\Bigg\} \\
&\quad + V\max\{P(t)\} \\
&\le \Phi + V\max\{P(t)\}.
\end{aligned}$$

Then we derive the upper bound of the *drift* $\Delta(L(t))$ as

$$\Delta(L(t)) \le \Phi + V\max\{P(t)\} - V\mathbb{E}\{P(t)\} \le \Phi + V\max\{P(t)\}$$

where $0 \le \Phi + V\max\{P(t)\} < \infty$. With the assumption that $\mathbb{E}\{A_i^u(t)\}^2 \le D$ and $\mathbb{E}\{A_i^d(t)\}^2 \le D$, for $i \in \mathcal{N}$, then we have

$$\mathbb{E}\Big\{\big|Q_i^u(t+1) - Q_i^u(t)\big|^2\Big\} \le \mathbb{E}\Big\{A_i^u(t)\Big\}^2 \le D, \text{for all } i \in \mathcal{N}.$$

Similarly, we have $\mathbb{E}\{|Q_i^u(t+1) - Q_i^u(t)|^2\} \le D$. According to [43, Proposition 3.1(b)], we have

$$\lim_{t\to\infty}\frac{Q(t)}{t} = 0. \tag{59}$$

## REFERENCES


[1] Z. Jiang and S. Mao, "Online channel assignment, transmission scheduling, and transmission mode selection in multi-channel full-duplex wireless LANs," in *Proc. 10th Int. Conf. Wireless Algorithms Syst. Appl. (WASA)*, vol. 9204. Qufu, China, Aug. 2015, pp. 243–252.

[2] J. I. Choi, M. Jain, K. Srinivasan, P. Levis, and S. Katti, "Achieving single channel, full duplex wireless communication," in *Proc. ACM MobiCom*, Chicago, IL, USA, Sep. 2010, pp. 1–12.

[3] D. Bharadia, E. McMilin, and S. Katti, "Full duplex radios," *ACM SIGCOMM Comput. Commun. Rev.*, vol. 43, no. 4, pp. 375–386, Oct. 2013.

[4] S. Gollakota and D. Katabi, "Zigzag decoding: Combating hidden terminals in wireless networks," in *Proc. ACM SIGCOMM*, Seattle, WA, USA, Aug. 2008, pp. 159–170.

[5] M. Jain *et al.*, "Practical, real-time, full duplex wireless," in *Proc. ACM MobiCom*, Las Vegas, NV, USA, Sep. 2011, pp. 301–312.

[6] M. Feng, S. Mao, and T. Jiang, "Duplex mode selection and channel allocation for full-duplex cognitive femtocell networks," in *Proc. IEEE WCNC*, New Orleans, LA, USA, Mar. 2015, pp. 1900–1905.

[7] M. Feng, S. Mao, and T. Jiang, "Joint duplex mode selection, channel allocation, and power control for full-duplex cognitive femtocell networks," *Elsevier Digit. Commun. Netw.*, vol. 1, no. 1, pp. 30–44, Feb. 2015.

[8] Y. Wang and S. Mao, "Distributed power control in full duplex wireless networks," in *Proc. IEEE WCNC*, New Orleans, LA, USA, Mar. 2015, pp. 1165–1170.

[9] Y. Wang and S. Mao, "On distributed power control in full duplex wireless networks," *Elsevier Digit. Commun. Netw. J.*, Nov. 2016, doi: 10.1016/j.dcan.2016.10.004.

[10] N. Tang, S. Mao, and S. Kompella, "Power control in full duplex underlay cognitive radio networks: A control theoretic approach," in *Proc. IEEE MILCOM*, Baltimore, MD, USA, Oct. 2014, pp. 949–954.

[11] N. Tang, S. Mao, and S. Kompella, "Power control in full duplex underlay cognitive radio networks," *Elsevier Ad Hoc Netw.*, vol. 37, pp. 183–194, Feb. 2016.

[12] S. Goyal *et al.*, "Improving small cell capacity with common-carrier full duplex radios," in *Proc. IEEE ICC*, Sydney, NSW, Australia, Jun. 2014, pp. 4987–4993.

[13] X. Xie and X. Zhang, "Does full-duplex double the capacity of wireless networks?" in *Proc. IEEE INFOCOM*, Toronto, ON, Canada, Apr./May 2014, pp. 253–261.

[14] M. J. Neely, E. Modiano, and C. E. Rohrs, "Dynamic power allocation and routing for time-varying wireless networks," *IEEE J. Sel. Areas Commun.*, vol. 23, no. 1, pp. 89–103, Jan. 2005.

[15] K. Kar, X. Luo, and S. Sarkar, "Throughput-optimal scheduling in multichannel access point networks under infrequent channel measurements," in *Proc. IEEE INFOCOM*, Anchorage, AK, USA, May 2007, pp. 1640–1648.

[16] Y. Huang, S. Mao, and R. M. Nelms, "Adaptive electricity scheduling in microgrids," *IEEE Trans. Smart Grid*, vol. 5, no. 1, pp. 270–281, Jan. 2014.

[17] M. J. Neely, *Stochastic Network Optimization With Application to Communication and Queueing Systems*, 1st ed. San Rafael, CA, USA: Morgan & Claypool, 2010.

[18] H. W. Kuhn, "The Hungarian method for the assignment problem," *Naval Res. Logist. Quart.*, vol. 2, nos. 1–2, pp. 83–97, Mar. 1955.

[19] H. Ju, E. Oh, and D. Hong, "Improving efficiency of resource usage in two-hop full duplex relay systems based on resource sharing and interference cancellation," *IEEE Trans. Wireless Commun.*, vol. 8, no. 8, pp. 3933–3938, Aug. 2009.

[20] T. Riihonen, S. Werner, and R. Wichman, "Optimized gain control for single-frequency relaying with loop interference," *IEEE Trans. Wireless Commun.*, vol. 8, no. 6, pp. 2801–2806, Jun. 2009.

[21] B. Debaillie *et al.*, "Analog/RF solutions enabling compact full-duplex radios," *IEEE J. Sel. Areas Commun.*, vol. 32, no. 9, pp. 1662–1673, Sep. 2014.

[22] S. Hong *et al.*, "Applications of self-interference cancellation in 5G and beyond," *IEEE Commun. Mag.*, vol. 52, no. 2, pp. 114–121, Feb. 2014.

[23] V. R. Cadambe and S. A. Jafar, "Degrees of freedom of wireless networks with relays, feedback, cooperation, and full duplex operation," *IEEE Trans. Inf. Theory*, vol. 55, no. 5, pp. 2334–2344, May 2009.
[24] C. S. Vaze and M. K. Varanasi, "The degrees of freedom of MIMO networks with full-duplex receiver cooperation but no CSIT," *IEEE Trans. Inf. Theory*, vol. 60, no. 9, pp. 5587–5596, Sep. 2014.
[25] D. Ramirez and B. Aazhang, "Optimal routing and power allocation for wireless networks with imperfect full-duplex nodes," *IEEE Trans. Wireless Commun.*, vol. 12, no. 9, pp. 4692–4704, Sep. 2013.
[26] K. Yang, H. Cui, L. Song, and Y. Li, "Joint relay and antenna selection for full-duplex AF relay networks," in *Proc. IEEE ICC*, Sydney, NSW, Australia, Jun. 2014, pp. 4454–4459.
[27] M. G. Khafagy, M.-S. Alouini, and S. Aissa, "Full-duplex opportunistic relay selection in future spectrum-sharing networks," in *Proc. IEEE ICCW*, London, U.K., Jun. 2015, pp. 1196–1200.
[28] G. Liu, F. R. Yu, H. Ji, V. C. M. Leung, and X. Li, "In-band full-duplex relaying: A survey, research issues and challenges," *IEEE Commun. Surveys Tuts.*, vol. 17, no. 2, pp. 500–524, 2nd Quart., 2015.
[29] Y. Cai, F. R. Yu, J. Li, Y. Zhou, and L. Lamont, "Medium access control for unmanned aerial vehicle (UAV) ad-hoc networks with full-duplex radios and multi-packet reception capability," *IEEE Trans. Veh. Technol.*, vol. 62, no. 1, pp. 390–394, Jan. 2013.
[30] N. Singh *et al.*, "Efficient and fair MAC for wireless networks with self-interference cancellation," in *Proc. WiOpt*, Princeton, NJ, USA, May 2011, pp. 94–101.
[31] K. Tamaki *et al.*, "Full duplex media access control for wireless multi-hop networks," in *Proc. IEEE VTC-Spring*, Dresden, Germany, Jun. 2013, pp. 1–5.
[32] W. Zhou, K. Srinivasan, and P. Sinha, "RCTC: Rapid concurrent transmission coordination in full duplex wireless networks," in *Proc. IEEE ICNP*, Göttingen, Germany, Oct. 2013, pp. 1–10.
[33] A. Tang and X. Wang, "A-duplex: Medium access control for efficient coexistence between full-duplex and half-duplex communications," *IEEE Trans. Wireless Commun.*, vol. 14, no. 10, pp. 5871–5885, Oct. 2015.
[34] J. Y. Kim, O. Mashayekhi, H. Qu, M. Kazadiieva, and P. Levis, "Janus: A novel MAC protocol for full duplex radio," Comput. Sci. Dept., Stanford Univ., Stanford, CA, USA, Tech. Rep. 2013-02, Jul. 2013.
[35] G. Chen, Y. Gong, P. Xiao, and J. A. Chambers, "Physical layer network security in the full-duplex relay system," *IEEE Trans. Inf. Forensics Security*, vol. 10, no. 3, pp. 574–583, Mar. 2015.
[36] H. Kim, S. Lim, H. Wang, and D. Hong, "Optimal power allocation and outage analysis for cognitive full duplex relay systems," *IEEE Trans. Wireless Commun.*, vol. 11, no. 10, pp. 3754–3765, Oct. 2012.
[37] X. Huang and N. Ansari, "Joint spectrum and power allocation for multi-node cooperative wireless systems," *IEEE Trans. Mobile Comput.*, vol. 14, no. 10, pp. 2034–2044, Oct. 2015.
[38] T. Han and N. Ansari, "A traffic load balancing framework for software-defined radio access networks powered by hybrid energy sources," *IEEE/ACM Trans. Netw.*, vol. 24, no. 2, pp. 1038–1051, Apr. 2016.
[39] Y.-J. Choi, S. Park, and S. Bahk, "Multichannel random access in OFDMA wireless networks," *IEEE J. Sel. Areas Commun.*, vol. 24, no. 3, pp. 603–613, Mar. 2006.
[40] E. Yaacoub and Z. Dawy, "A survey on uplink resource allocation in OFDMA wireless networks," *IEEE Commun. Surveys Tuts.*, vol. 14, no. 2, pp. 322–337, 2nd Quart., 2012.
[41] C. Nam, C. Joo, and S. Bahk, "Joint subcarrier assignment and power allocation in full-duplex OFDMA networks," *IEEE Trans. Wireless Commun.*, vol. 14, no. 6, pp. 3108–3119, Jun. 2015.
[42] Z. Jiang and S. Mao, "Energy delay tradeoff in cloud offloading for multi-core mobile devices," *IEEE Access*, vol. 3, pp. 2306–2316, 2015.
[43] M. J. Neely, "Stability and probability 1 convergence for queueing networks via Lyapunov optimization," *J. Appl. Math.*, vol. 2012, Apr. 2012, Art. no. 831909.
[44] M. Gong, S. F. Midkiff, and S. Mao, "Design principles for distributed channel assignment in wireless ad hoc networks," in *Proc. IEEE ICC*, Seoul, South Korea, May 2005, pp. 3401–3406.

**Zhefeng Jiang** (S'15) received the bachelor's degree in electrical engineering from Beijing Jiaotong University, Beijing, China, in 2009, the master's degree in electrical engineering from Tsinghua University, Beijing, in 2012, and the Ph.D. degree in electrical and computer engineering from Auburn University, Auburn, AL, USA, in 2016.

He has been a Software Engineer with Google Inc., Mountain View, CA, USA, since 2016. His current research interests include cognitive radios, cloud computing, full-duplex wireless networks, and LTE in unlicensed bands.

**Shiwen Mao** (S'99–M'04–SM'09) received the Ph.D. degree in electrical and computer engineering from Polytechnic University (now Tandon School of Engineering of New York University), Brooklyn, NY, USA, in 2004.

He is currently the Samuel Ginn Distinguished Professor and the Director of the Wireless Engineering Research and Education Center, Auburn University, Auburn, AL, USA. His current research interests include wireless networks and multimedia communications.

Dr. Mao was a recipient of the 2015 IEEE ComSoc TC-CSR Distinguished Service Award, the 2013 IEEE ComSoc MMTC Outstanding Leadership Award, and the NSF CAREER Award in 2010. He was a co-recipient of the Best Paper Awards from the IEEE GLOBECOM 2015 and 2016, the IEEE WCNC 2015, and the IEEE ICC 2013, and the 2004 IEEE Communications Society Leonard G. Abraham Prize in the field of communications systems. He is a Distinguished Lecturer of the IEEE Vehicular Technology Society. He is on the Editorial Board of the IEEE TRANSACTIONS ON MULTIMEDIA, the IEEE INTERNET OF THINGS JOURNAL, and IEEE MULTIMEDIA. He serves as the TPC Chair of the IEEE INFOCOM 2018, the Area TPC Chair of the IEEE INFOCOM 2016 and 2017, the Technical Program Vice Chair for Information Systems (EDAS) of the IEEE INFOCOM 2015, the Symposium Co-Chairs for several conferences, including the IEEE ICC, the IEEE GLOBECOM, and ICCCN, a Steering Committee Voting Member for the IEEE ICME and AdhocNets, and various roles in the organizing committees of several conferences. He is the Chair of the IEEE ComSoc Multimedia Communications Technical Committee.